Chemistry and Physics of Lipids 201 (2016) 1–10

Contents lists available at ScienceDirect

Chemistry and Physics of Lipids

journal homepage: www.elsevier.com/locate/chemphyslip

Structure, supramolecular organization and phase behavior of *N*-acyl-β-alanines: Structural homologues of mammalian brain constituents *N*-acylglycine and *N*-acyl-GABA

D. Sivaramakrishna, Musti J. Swamy*

School of Chemistry, University of Hyderabad, Hyderabad-500 046, India

ARTICLE INFO

Article history:
Received 25 August 2016
Received in revised form 29 September 2016
Accepted 15 October 2016
Available online 19 October 2016

Keywords:
N-acyl amino acid
Differential scanning calorimetry
Thermotropic phase transition
X-ray diffraction
Tilted bilayer
Odd-even alternation

ABSTRACT

N-Acyl-β-alanines (NABAs) are structural homologues of *N*-acylglycines (NAGs) and *N*-acyl-γ-amino-butyric acids (NAGABAs), and achiral isomers of *N*-acylalanines, which are all present in mammalian brain and other tissues and modulate activity of biological receptors with various functions. In the present study, we synthesized and characterized a homologous series of NABAs bearing saturated acyl chains (n = 8-20) and investigated their supramolecular organization and thermotropic phase behavior. In differential scanning calorimetric (DSC) studies, most of the NABAs gave one or two minor transitions before the main chain-melting phase transition in the dry state as well as upon hydration with water, but gave only a single transition when hydrated with buffer (pH 7.6). Transition enthalpies (ΔH_t) and entropies (ΔS_t), obtained from the DSC studies showed linear dependence on the chain length in the dry state and upon hydration with buffer, whereas odd-even alteration was observed when hydrated with water. The crystal structures of *N*-lauroyl-β-alanine (NLBA) and *N*-myristoyl-β-alanine (NMBA) were solved in monoclinic system in the P21/*c* space group. Both NLBA and NMBA were packed in tilted bilayers with head-to-head (and tail-to-tail) arrangement with tilt angles of 33.28° and 34.42°, respectively. Strong hydrogen bonding interactions between —COOH groups of the molecules from opposite leaflets as well as N—H···O hydrogen bonds between the amide groups from adjacent molecules in the same leaflet as well as dispersion interactions between the acyl chains stabilize the bilayer structure. The *d*-spacings calculated from powder X-ray diffraction studies showed odd-even alteration with odd-chain length compounds exhibiting higher values as compared to the even-chain length ones and the tilt angles calculated from the PXRD data are higher for the even chain NABAs. These observations are relevant to developing structure-activity relationships for these amphiphiles and understand how NABAs differ from their homologues and isomers, namely NAGs, NAGABAs, and *N*-acylalanines.

1. Introduction

β-Alanine, a naturally occurring β-amino acid, shows agonist activity towards glycine receptors and γ-amino acid receptors (Schmieden et al., 1993; Mori et al., 2002; Horikoshi et al., 1988). It is formed *in vivo* by degradation of dihydrouracil and carnosine. β-Alanine is a component of the natural peptides carnosine and anserine as well as vitamin B_5 and coenzyme A. Carnosine levels depend on the available amount of β-alanine; supplementation increases the carnosine levels in muscle, decreases fatigue in athletes and increases the total muscular work done (Harris et al., 2006; Hill et al., 2007; Derave et al., 2007). Due to the β-amino group, β-alanine is not incorporated into proteins; therefore it is stored in relatively larger amounts in muscles and forms dipeptides with L-histidine and acts as an intramuscular buffer with 10–20% of the total buffering capacity in type I and type II muscle fibers (Smith, 1938). It also acts as an agonist of strychnine-sensitive inhibitory glycine receptors (Curtis et al., 1968; Davidoff et al., 1969).

N-Acyl conjugates of amino acids (*N*-acyl amino acids, NAAs) are a new class of lipids, which are found in mammalian brain and other tissues with significant biological properties (Huang et al., 2001; Chu et al., 2003; Saghatelian et al., 2006; Milman et al., 2006; Rimmerman et al., 2008; Bradshaw et al., 2006, 2009; Tan et al., 2010). They act as endogenous ligands for cannabinoid receptors

* Corresponding author.
E-mail addresses: mjswamy@uohyd.ac.in, mjswamy1@gmail.com (M.J. Swamy).

http://dx.doi.org/10.1016/j.chemphyslip.2016.10.002
0009-3084/

and inhibit transporters with different functions (Wiles et al., 2006). They show varying degrees of potency towards *T*-type and *N*-type calcium ion channel currents (Guo et al., 2008), and show different activity (inhibition/enhancement) of fatty acid amide hydrolase (Cascio et al., 2004).

In addition to the above interesting biological properties, NAAs also exhibit considerable potential for use in various applications. For example, *N*-acyl derivatives of carnosine and histidine act as antioxidants and emulsifying agents (Murase et al., 1993), whereas *N*-acylphenylalanine and *N*-acylmethionine altered the thermal stability, foaming stability, emulsifying activity and gelation properties of food ingredients such as egg white and whey protein (Ma et al., 1993). *N*-Acyl amino acids and *N*-acyl amino acid esters form gels in organic solvents and selectively form gels in oil-water mixtures (Duarte et al., 2012). In view of their biodegradable and non-toxic nature they can potentially be used in drug delivery applications (Vintiloiu et al., 2008).

In view of the foregoing, it is important to investigate NAAs in a systematic manner in order to understand their physicochemical properties, phase behavior and interaction with other amphiphiles in order to utilize them in various applications. In this direction we have recently reported the thermotropic phase behavior, 3-dimensional structure and supramolecular assembly of *N*-acylglycines (NAGs) (Reddy et al., 2014) and *N*-acyl L-alanines (NAAlas) (Sivaramakrishna et al., 2015) which are constituents of mammalian brain. In the present study we have focused our attention on *N*-acyl β-alanines (NABAs), which are homologues of NAGs and achiral isomers of NAAlas. We have synthesized a homologous series of NABAs bearing saturated acyl chains (n = 8–20), investigated their phase transitions in the dry state and upon complete hydration (water and phosphate buffer) by differential scanning calorimetry. Crystal structures of two representatives, namely *N*-lauroyl β-alanine (NLBA) and *N*-myristoyl β-alanine (NMBA) have been determined by single-crystal X-ray diffraction and analyzed the molecular packing and intermolecular interactions have been analyzed. The results obtained are discussed in this report.

2. Experimental section

2.1. Materials

β-Alanine ethyl ester hydrochloride and long chain fatty acids (CH_3 $(CH_2)_n$ COOH, n = 6–18) were purchased from Sigma-Aldrich (Milwaukee, WI, USA). Oxalyl chloride was purchased from Merck (Germany). Other chemicals and solvents (analytical grade) were purchased from local chemical suppliers.

2.2. Synthesis of N-acyl β-alanines

NABAs were prepared by a procedure that is essentially similar to that reported for the synthesis of NAAlas (Sivaramakrishna et al., 2015). First, fatty acyl chlorides were prepared from the corresponding fatty acids (1 mol eq.) by treating with oxalyl chloride as described earlier (Akoka et al., 1988). β-Alanine ethyl ester hydrochloride (1 mol eq.) and sodium bicarbonate (2 mol eq.) were dissolved in about 5 ml of distilled water, stirred for 5–10 min and 10 ml of chloroform was added. After stirring for 10–15 min at room temperature, the acid chloride, dissolved in chloroform, was added dropwise and the reaction mixture was kept under constant stirring for 3 h. The *N*-acyl β-alanine ethyl ester obtained was extracted with chloroform and washed successively with the double distilled water, saturated brine solution, 0.1 M HCl and double distilled water. The solid *N*-acyl-β-alanine ethyl esters obtained after evaporating the solvent were taken in MeOH:H_2O (3:1, v/v) and hydrolyzed with LiOH by overnight stirring. Then the reaction mixtures were acidified with 2 M HCl and the *N*-acyl β-alanines were extracted with ethyl acetate. The extract was washed successively with 0.1 M HCl and double distilled water. The product obtained was recrystallized from hexane (for n = 8, 9) or ethyl acetate (for n = 10–20). The overall yield for different NABAs ranged around 70–80%. The final products were characterized by thin layer chromatography, FTIR, ^{1}H and ^{13}C NMR spectroscopy as well as by high resolution mass spectrometry.

Melting points were determined using a Superfit (Mumbai, India) melting point apparatus. FTIR spectra were recorded using KBr pellets on a Jasco FTIR 5300 Spectrometer. ^{1}H and ^{13}C NMR spectra were recorded on a Bruker Avance NMR spectrometer at 400 and 100 MHz, respectively. $CDCl_3$ was used as the solvent for all ^{1}H NMR as well as ^{13}C NMR spectral studies with shorter chain NABAs (8–10), whereas $CDCl_3$ containing a few drops of CD_3OD was used as the solvent for longer chain NABAs. High-resolution ESI mass spectra for NABAs with 8–20 C-atoms in the acyl chain were recorded in the positive ion mode on a Bruker MaXis Mass Spectrometer.

2.3. DSC of dry N-acyl-β-alanines

DSC experiments with dry NABAs were carried out on a Perkin-Elmer Pyris Diamond differential scanning calorimeter. The dry compounds were accurately weighed using a microbalance (Perkin-Elmer) in aluminum sample pans, covered with lids and sealed by crimping. Each sample was subjected to three heating and two cooling scans at a scan rate of 2°/min. After the 1st heating scan, small changes were observed in the minor transition peak intensity and peak positions, whereas second and third heating thermograms were almost identical. Therefore, the second heating scans were considered for further analysis of all samples. Transition enthalpies (ΔH_t) were obtained by integrating the peak area under the transition curve using the software provided by the instrument manufacturer. Transition entropies (ΔS_t) were calculated from the transition enthalpies assuming a first order transition according to equation 1 (Marsh, 1990).

$$\Delta S_t = \Delta H_t / T_t \quad (1)$$

where T_t refers to the transition temperature.

2.4. DSC of hydrated N-acyl-β-alanines

DSC studies with hydrated samples were performed using a VP-DSC equipment from Microcal LLC (Northampton, MA, USA). Accurately weighed compounds (~4–5 mg each) were dissolved in about 300 μl chloroform containing a drop of methanol and the solvent was evaporated by blowing a gentle stream of dry N_2 gas. The lipid films thus obtained were vacuum desiccated for 5–6 h and then hydrated with double distilled water or 20 mM phosphate buffer, pH 7.6, containing 1 M NaCl (PBS) by subjecting the sample through 4–5 cycles of freeze-thawing. To get a homogenous mixture, the samples were sonicated for 1–2 min. Heating scans were recorded from 10 to 120 °C at a scan rate of 60°/h. Three heating and two cooling scans were performed for each sample. The transition enthalpy was found to decrease in the second and third heating scans. Therefore, the first heating scans were considered for further analysis. Transition temperatures, enthalpies and width at half height were determined using the Origin software provided by the calorimeter. Transition entropies were calculated from the transition enthalpies assuming a first order transition according to Eq. (1).

2.5. Crystallization and X-ray diffraction

Thin plate-type, colorless single crystals of NLBA and NMBA were grown at room temperature from ethyl acetate containing a

trace of methanol or ethanol. X-ray diffraction data were collected at room temperature (~25 °C) on an Oxford Gemini X-ray diffractometer equipped with Cu-Kα radiation source (λ = 1.5418 Å). Crystal parameters for both NLBA and NMBA are given in Table 1.

2.6. Structure solution and refinement

For NLBA and NMBA the data collected in the range of θ = 3.74-69.44° and θ = 3.35–71.42°, respectively, were used for structure solution. Data reduction was done using CrysAlisPro 171.36.28 software and crystal structure was solved and refined using Olex2-1.0 program and absorption correction was not done. Both structures were solved in the monoclinic crystal system with $P2_1/c$ space group. For NLBA the refinement was carried out using 4907 observed [>2σ (F_0)] reflections, which converged into final R_1 = 0.0942, wR_2 = 0.2637 and goodness of fit = 1.062. For NMBA the refinement was carried out using 3419 observed [>2σ (F_0)] reflections, which converged into final R_1 = 0.0759, wR_2 = 0.2393 and goodness of fit = 1.121.

2.7. Powder X-ray diffraction studies

Powder X-ray diffraction patterns of NABAs were recorded on a Bruker SMART D8 Advance powder X-ray diffractometer (Bruker-AXS, Karlsruhe, Germany) with Cu-Kα radiation at 40 kV and 30 mA. Fine powders of the NABAs, obtained by grinding with mortar and pestle, were placed on a circular rotating disk of the sample holder of the instrument. Diffraction patterns were collected at room temperature using a LynxEye PSD data collector over a 2θ range of 1–50° with a step size of 0.0198° and a measuring time of 1.5 s for each step.

3. Results and discussion

The *N*-acyl-β-alanines synthesized in the present study were broadly characterized by various spectroscopic methods (FTIR, ^{1}H- and ^{13}C NMR) as well as by high-resolution mass spectrometry, and the details are given in the Supporting information (Figs. S1–S4, Tables S1–S4). Results of the above spectral analyses are fully consistent with the structures of *N*-acyl-β-alanines and indicate that they are all highly pure.

Table 1
Crystallographic data for *N*-lauroyl-β-alanine and *N*-myristoyl-β-alanine at 298 K.

Crystal parameter	NLBA	NMBA
Formula	$C_{15}H_{29}NO_3$	$C_{17}H_{33}NO_3$
Formula wt.	271.39	299.44
Crystal system	Monoclinic	Monoclinic
T, °C	25	25
Space group	*P*21/*c*	*P*21/*c*
a (Å)	35.665 (3)	39.740 (4)
b (Å)	4.860 (4)	4.866 (3)
c (Å)	9.276 (7)	9.240 (5)
α	90.00	90.00
β	94.34 (9)	90.381 (6)
γ	90.00	90.00
Z	4	4
V (Å^3)	1603.4 (2)	1786.5 (2)
D_{calc} (g cm^{-3})	1.124	1.113
μ (mm^{-1})	0.612	0.590
F(000)	600	664
Total Reflections	3120	3419
Used Reflections	1811	2202
Parameters	174	192
GOF	1.062	1.121
R indices (all data)	R_1 = 13.22, wR_2 = 29.42	R_1 = 8.29, wR_2 = 24.92
Final R indices	R_1 = 9.42, wR_2 = 26.41	R_1 = 7.59, wR_2 = 23.92

3.1. DSC of dry *N*-acyl-β-alanines

Three successive heating thermograms of dry *N*-undecanoyl-β-alanine (NUBA, bearing 11 C-atoms in the acyl chain) and *N*-myristoyl-β-alanine (NMBA, bearing 14 C-atoms in the acyl chain) are shown in Figs. 1A and 1B. First and second heating thermograms of all dry NABAs are shown in Fig. S5 and S6, respectively. The heating thermograms presented in Figs. 1A, B and Figs. S5 and S6 show that all dry NABAs exhibit one or two minor transitions before the major, melting transition in the first heating scan. The minor transitions correspond to solid–solid phase transitions and indicate the possibility of polymorphism in the compounds. Interestingly, in the second and third heating scans, one of the additional transitions disappeared in the thermograms corresponding to *N*-lauroyl and *N*-palmitoyl compounds, whereas both minor transitions were seen in the thermograms of *N*-(nonanoyl, undecanoyl and pentadecanoyl) compounds in further heating scans. Moreover, peaks corresponding to the minor transitions shifted to lower temperatures, accompanied, in most cases, by considerable sharpening in the second and third heating scans as compared to the first heating scan. *N*-Decanoyl and *N*-tridecanoyl compounds showed only one minor transition in the second and third heating scans as compared to two transitions in the first heating scan. Changes in the minor peak position are listed in Table S8. The above observations suggest that during cooling some of the NABAs do not come back to the structure of initial starting form. Since the second and third heating scans gave reproducible results, in all cases, data from second heating scans were considered for further analysis. Transition enthalpies were obtained by integrating the total area under the major and minor transitions. Transition temperatures (T_t), transition enthalpies (ΔH_t) and transition entropies (ΔS_t) obtained from the first heating thermograms are shown in Table S5 and ΔH_t and ΔS_t values obtained from the second heating thermograms are presented in Table S6.

3.2. DSC of hydrated N-acyl-β-alanines

Three successive heating thermograms of NUBA and NMBA hydrated with water are shown in Fig. 1C and 1D, respectively and first and second heating thermograms of the homologues series of NABAs hydrated with water are shown in Fig. S8 and Fig. S9, respectively. These thermograms show that most of the NABAs investigated here exhibit one minor transition before the major, chain-melting transition in the hydrated state. The only exceptions are *N*-decanoyl β-alanine which shows two minor transitions in all the heating scans, *N*-tridecanoyl-β-alanine which shows two minor transitions in the first heating scan but three minor transitions in the subsequent heating scans, and *N*-pentadecanoyl β-alanine which shows one minor transition in the first heating scan but two minor transitions in the subsequent heating scans. For some single chain amphiphiles such as *N*-acylethanolamines (Ramakrishnan et al., 1997; Ramakrishnan and Swamy, 1998) and *N*-acylglycines (Reddy et al., 2014) it was observed the minor transitions seen in the dry state disappear upon hydration, but in the present case not only minor transitions are observed in the hydrated state but they become sharper in the second and third heating cycles as observed in the dry state (see above). However, transition enthalpies were found to decrease slightly (< 10%) in the second and third heating scans, as compared to the first heating scan. Therefore, in all cases, the first heating scan was considered

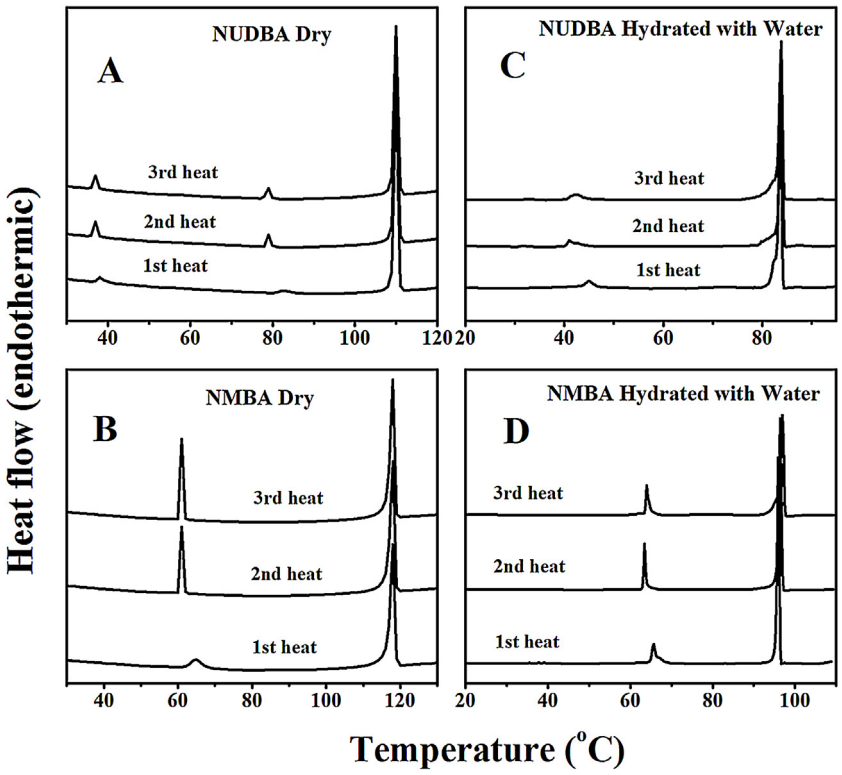

Fig. 1. DSC thermograms of *N*-undecanoyl-β-alanine and *N*-myristoyl-β-alanine in dry (A, B) and hydrated (C, D) states. Thermograms corresponding to three successive heating cycles are shown.

for further analysis. Values of ΔH_t and ΔS_t (combined values for the major and minor transitions) obtained from the first heating thermograms are given in Table S6 and the T_t values are given in Table S7, whereas temperatures corresponding to the minor transitions are listed in Table S8.

Thermograms of NABAs ($n = 10–20$) hydrated with buffer (Figs. 2A, 2B) show that each compound exhibits a single sharp transition peak at a temperature well below the phase transition temperature of the dry samples as well as those hydrated with water. When the samples were subjected to a second and third heating scan, small decreases were observed in the transition

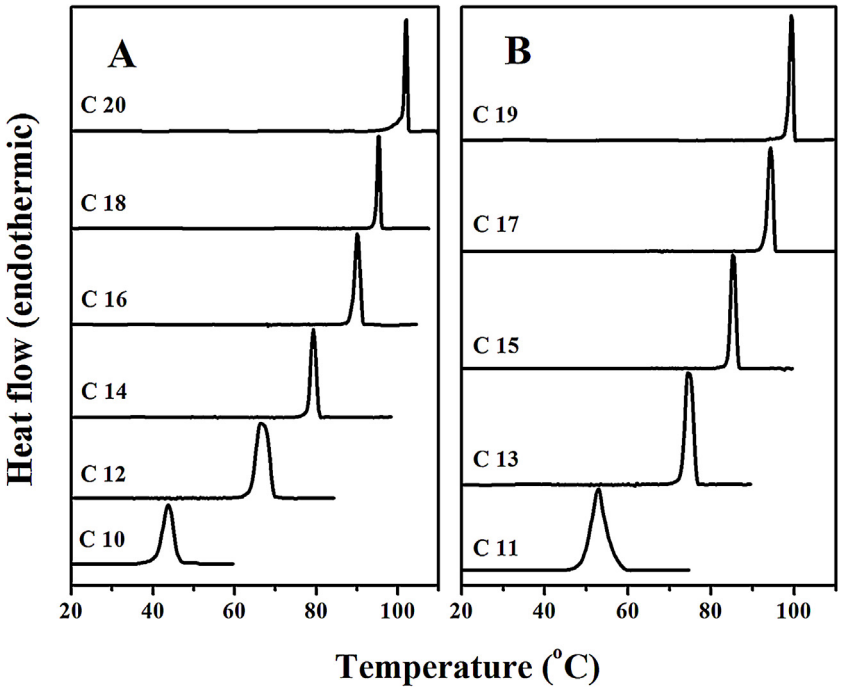

Fig. 2. DSC thermograms corresponding to the first heating scan of *N*-acyl-β-alanines hydrated with phosphate buffer, pH 7.6, containing 1 M NaCl. The number of C-atoms in the acyl chains is indicated against each thermogram.

enthalpies as compared to the values obtained from the first scan. Therefore, in all cases, the first heating scan was considered for further analysis and values of ΔH_t and ΔS_t obtained are given in Table S6 and the T_t values are given in Table S7.

3.3. Chain length dependence of transition enthalpy and entropy

Chain length dependence of the transition enthalpy (ΔH_t) and transition entropy (ΔS_t) of dry NABAs obtained from the first heating scans are given in Fig. S7. Plots of total ΔH_t and ΔS_t (sum of major and minor transitions) versus chain length are shown in Figs. S7A, S7B, respectively, whereas plots of ΔH_t and ΔS_t corresponding to the major transitions alone are shown in Figs. S7C, S7D, respectively. In both cases no clear pattern was observed in the ΔH_t and ΔS_t values with increasing acyl chain length. However, values of both ΔH_t and ΔS_t determined from the second heating scans exhibit linear dependence on the chainlength (Fig. 3A, B, filled circles). Similar linear chainlength dependence of ΔH_t and ΔS_t was reported earlier for *N*-acylglycines, which are homologous to NABAs with one CH_2 group less in the head group. The enthalpy and entropy data obtained from the second heating for NABAs could be fit well to expressions (2) and (3) given below as observed previously with *N*-acylglycines, *N*-acyl L-alanines, *N*-acylethanolamines, *N*, *O*-diacylethanolamines, L-alanine alkyl esters, *N*-acyl L-alanine alkyl esters, *N*-acyl L-alaninols, *N*-acyldopamines and *N*-acylserotonins (Reddy et al., 2014, 2013; Sivaramakrishna et al., 2015; Ramakrishnan et al., 1997; Kamlekar et al., 2010; Sivaramakrishna and Swamy, 2015a,b, 2016; Reddy and Swamy, 2015):

$$\Delta H_t = \Delta H_o + (n-2)\ \Delta H_{inc} \quad (2)$$

$$\Delta S_t = \Delta S_o + (n-2)\ \Delta S_{inc} \quad (3)$$

where ΔH_{inc} and ΔS_{inc} are the incremental values of transition enthalpy and transition entropy per CH_2 group. ΔH_o and ΔS_o are the end contributions to ΔH_t and ΔS_t, respectively, arising from the methyl group of the acyl chain and the head group region. Values of ΔH_o, ΔS_o, ΔH_{inc} and ΔS_{inc}, for the NABAs obtained from linear least squares analysis, are given in Table 2. A linear chain length dependence of the transition enthalpy and transition entropy observed here for the dry NABAs indicates that the structures of NABAs are very similar in the solid state. Therefore molecular packing and intermolecular interactions in all the NABAs are expected to be rather similar and determination of the 3-dimensional structure of any member of the series can give a good idea of the molecular packing and intermolecular interactions present in the crystal lattice of all the NABAs.

Chainlength dependence of ΔH_t and ΔS_t of NABAs hydrated with PBS is shown in Fig. 3A, B (open circles), respectively. Similar to the dry samples (second heat), values of transition enthalpy and entropy exhibit a linear dependence on the chainlength for $n = 11$–20. Fitting the ΔH_t and ΔS_t values to Eqs. (2) and (3) yielded the incremental values (ΔH_{inc}, ΔS_{inc}) and end contributions (ΔH_o, ΔS_o), which are presented in Table 2. In contrast to the linear dependence of the transition enthalpy and entropy seen with dry and buffer-hydrated NABAs, ΔH_t and ΔS_t values corresponding to NABAs that were hydrated with water show odd-even alteration (Fig. 3C, D) with the odd chain compounds having lower values as compared to the even chain compounds (except *N*-octanoyl-β-alanine which has the shortest acyl chain). While NABAs exhibit linear dependence of ΔH_t and ΔS_t on the acyl chain length in the dry state and upon hydration with PBS, interestingly, upon hydration with water they exhibit an odd-even alteration, with linear dependence of ΔH_t and ΔS_t being observed independently

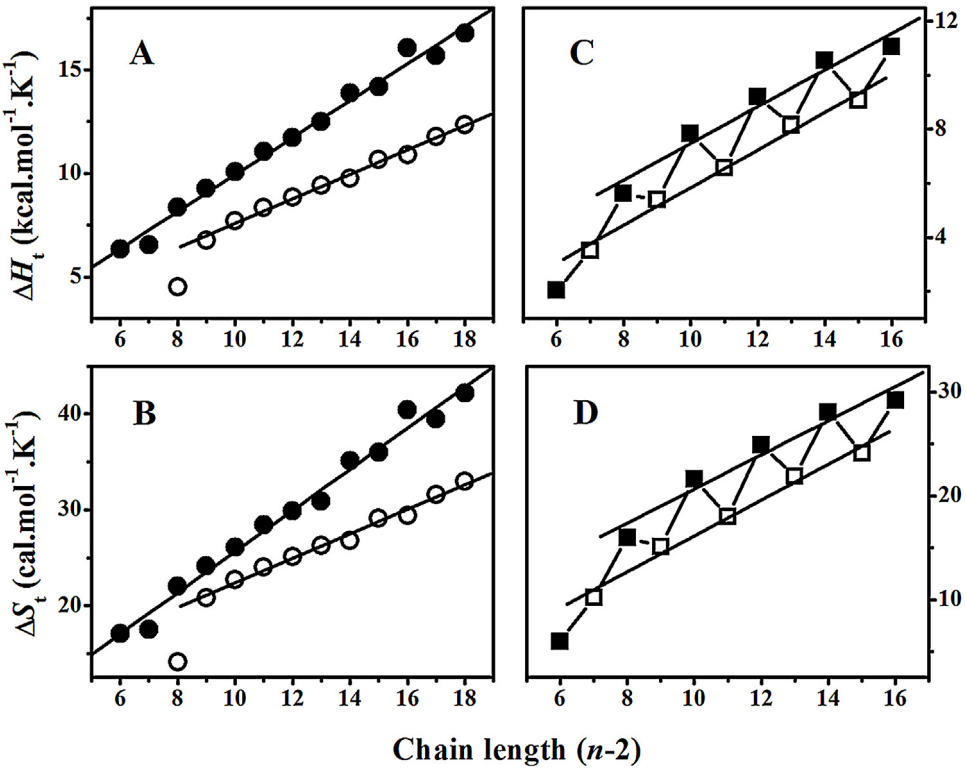

Fig. 3. Chain length dependence of transition enthalpy and transition entropy of NABAs in the dry state and upon hydration with water and PBS. A, C) Transition enthalpy; B, D) transition entropy. Filled circles (●), dry samples (second heating scan); open circles (○), samples hydrated with 20 mM phosphate buffer, pH 7.6, containing 1 M NaCl (PBS). Filled squares (■), even chain length NABAs hydrated with water; open squares (□), odd chain length NABAs hydrated with water. Values of ΔH_t and ΔS_t were plotted against the number of methylene (CH_2) units (*n*-2). Solid lines correspond to linear least squares fits of the data. For more details see the text.

Table 2
Incremental values (ΔH_{inc}, ΔS_{inc}) of chain length dependence and end contributions (ΔHo, ΔSo) to phase transition enthalpy and entropy of *N*-acyl β-alanines in the dry state and upon complete hydration with water and phosphate buffer, pH 7.6, containing 1 M NaCl (PBS). Values in parentheses correspond to fitting errors obtained from the least squares analysis.

Thermodynamic parameter	Dry NABAs	NABAs hydrated with PBS	NABAs hydrated with water	
			Even chain length	Odd chain length
ΔH_{inc} (kcal/mol)	0.89 (0.03)	0.59 (0.02)	0.68 (0.08)	0.70 (0.04)
ΔH_o (kcal/mol)	1.01 (0.37)	1.71 (0.25)	0.7 (1.04)	−1.11 (0.48)
ΔS_{inc} (cal/mol/K)	2.14 (0.08)	1.28 (0.05)	1.64 (0.23)	1.73 (0.12)
ΔS_o (cal/mol/K)	4.20 (0.97)	9.57 (0.67)	4.22 (2.79)	−1.17 (1.41)

for the odd- and even-chain series (Fig. 3C, D). End contributions (ΔH_o, ΔS_o) and incremental values (ΔH_{inc} and ΔS_{inc}) for the odd- and even-chainlength series of hydrated NABAs obtained from the linear least squares fits are also given in Table 2. This suggests that while the phase structure of all members of the homologous series and the intermolecular interactions exhibited by them when hydrated with PBS (where they are all in the anionic form) would be expected to be rather similar, differences exist in the phase structure and/or intermolecular interactions in the odd- and even chain length series compounds when hydrated with water (where they exist in the neutral form).

Generally thermodynamic parameters for the even chain length series are higher as compared to those of the odd chain length series, as observed previously for long chain carboxylic acids, *N*-acylethanolamines, *N*, *O*-diacylethanolamines, *N*-acyldopamines and *N*-acylserotonins (Ramakrishnan et al., 1997; Kamlekar et al., 2010; Reddy et al., 2013; Reddy and Swamy, 2015; Larsson, 1986; Tarafdar et al., 2012). In a few cases, the odd chain length series exhibits higher values as compared to the even chain series. Examples of this category include *N*-acyl L-alanines, *N*-acyl-L-alanine esters with matched acyl and alkyl chains in dry state, phosphatidylcholines bearing ω-tertiary-butyl fatty acyl chains or *dl*-methyl anteisobranched fatty acyl chains in the hydrated state (Sivaramakrishna et al., 2015; Sivaramakrishna and Swamy, 2015a; Lewis et al., 1987, 1989).

3.4. Chain length dependence of transition temperature

Chainlength dependence of transition temperatures of NABAs in the dry state, and upon complete hydration with water as well as PBS are given in Fig. 4. The transition temperatures in each case

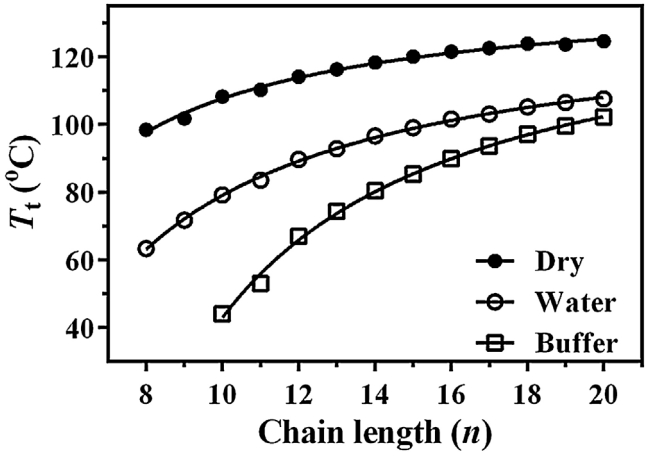

Fig. 4. Chain length dependence of chain-melting phase transition temperatures of NABAs. Filled circles (●), dry samples; open circles (○), hydrated with water; open squares (□), hydrated with 20 mM phosphate buffer, pH 7.6, containing 1 M NaCl. Solid lines correspond to nonlinear least-squares fit of the transition temperatures to eq 7.

increase in a smooth progression although the increments between successive values decrease with increase in the chain length. For each compound, the T_t value is highest in the dry state and lowest when hydrated with PBS, whereas the value is intermediate when hydrated with water. Thus, the T_t of *N*-decanoyl-β-alanine with the shortest acyl chain is 108.2 °C, 79.2 °C and 44 °C in the dry state, upon hydration with water and buffer, respectively, whereas the corresponding values for *N*-arachidonyl-β-alanine with the longest acyl chain are 124.6 °C, 107.6 °C and 102.2 °C, respectively. As the acyl chainlength increases, end contributions towards the total enthalpy and entropy of the phase transition become relatively very small compared to those from the polymethylene chain portion; hence, they can be neglected in comparison. Therefore, at infinite acyl chainlength, Eqs. (2) and (3) can be simplified by neglecting the end contributions and written as (4) and (5):

$$\Delta H_t = (n\text{-}2)\ \Delta H_{inc} \quad (4)$$

$$\Delta S_t = (n\text{-}2)\ \Delta S_{inc} \quad (5)$$

The transition temperature at infinite chainlength, T_t^∞, can then be obtained from the ratio $\Delta H_{inc}/\Delta S_{inc}$. Using this relationship, the T_t^∞ values were estimated as 415.9 K and 460.9 K for NABAs in the dry state and upon hydration with phosphate buffer, respectively, and as 414.6 K and 404.6 K, respectively, for even- and odd-chainlength NABAs upon hydration with water.

For a variety of amphiphiles with one/two hydrophobic chains that exhibit linear dependence of ΔH_t and ΔS_t on the chain length, these thermodynamic parameters obey the following equation (Marsh, 1982):

$$T_t = \Delta H_t/\Delta S_t = T_t^\infty\ [1-(n_o\text{-}n'_o)/(n\text{-}n'_o)] \quad (6)$$

where $n_o(=-\Delta H_o/\Delta H_{inc})$ and $n'_o(=-\Delta S_o/\Delta S_{inc})$ are the values of n at which the transition enthalpy and transition entropy extrapolate to zero. It can be seen from Fig. 4 that the T_t values of both dry and hydrated NABAs fit quite well to Eq. (6). Besides, the fitting parameters yielded the T_t^∞ values for NABAs in the dry state as 413.3 K, upon hydration with water as 406.6 K and upon hydration with buffer as 414.6 K. The value obtained for dry and hydrated (with water) NABAs are in good agreement with the T_t^∞ values estimated from the $\Delta H_{inc}/\Delta S_{inc}$ ratio.

3.5. Description of the structures

Molecular structures of NLBA and NMBA, determined by single-crystal X-ray diffraction are shown in the ORTEPs given in Fig. 5A and Fig. 5B, respectively, along with the atom numbering for all non-hydrogen atoms. The corresponding atomic coordinates and equivalent isotropic displacements as well as bond distances, bond angles and torsion angles are given in Tables S9-S11 and S12-S14, respectively. These data show that the hydrocarbon portion of the acyl chains of NLBA (C2-C12) and NMBA (C2-C14) are in all-trans conformation with all the torsion angles being ~180°. The torsion

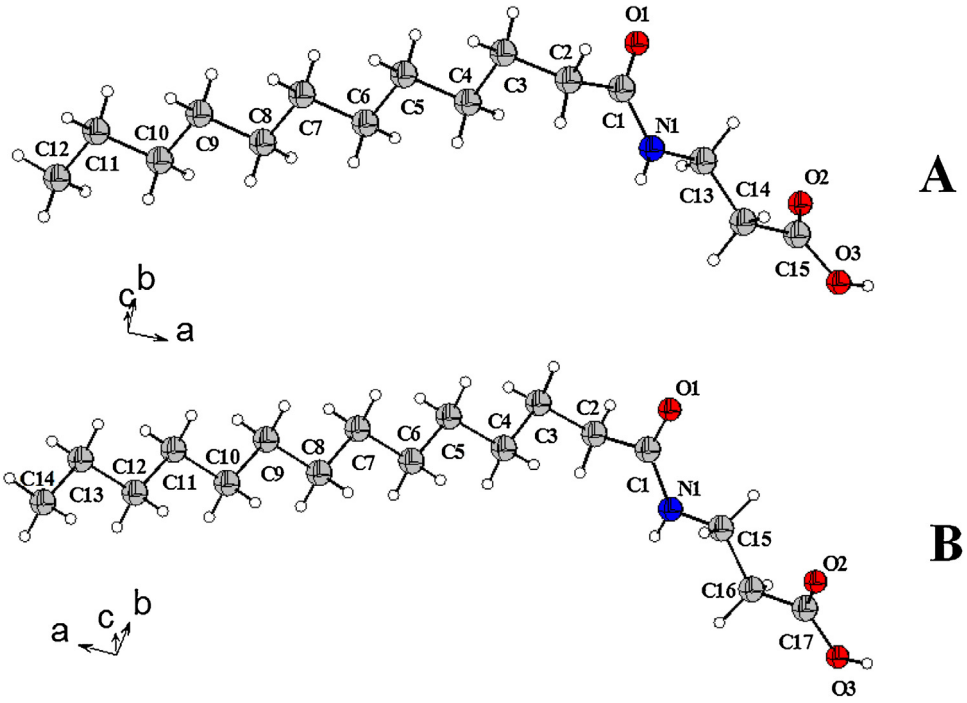

Fig. 5. ORTEPs showing the molecular structures of *N*-lauroyl-β-alanine (A) and *N*-myristoyl-β-alanine (B).

angles corresponding to the N1-C1-C2-C3 linkage in NLBA and NMBA are −128.1° and 128.8°, respectively. The torsion angles observed for C1-C2-C3-C4 linkage in NLBA and NMBA are 67.7° and −68°, respectively. The gauche conformation at the C2-C3 bond results in a bending of the molecule, giving it 'L' shape. The amide N—H and carbonyl group are also in the trans geometry.

3.6. Molecular packing

Packing diagrams of NLBA and NMBA along the *b*-axis are given in Fig. 6A and B, respectively, whereas the packing diagrams along the *c*-axis are given in Fig. S10A and Fig. S10B, respectively. Both molecules are packed in a bilayer format with head-to-head orientation of the carboxylic acid groups, which associate via O—H···O hydrogen bonds, leading to the formation of carboxylic acid dimers that connect adjacent bilayers (Fig. 6C). In addition, amide groups from adjacent molecules in the same leaflet are also involved in hydrogen bonding (Fig. 6D). The carbonyl oxygen atoms of the amide moieties of adjacent molecules point in opposite directions such that the adjacent hydrogen-bonded chains run in opposite directions. The methyl ends of stacked bilayers are in van der Waals' contacts, with the closest methyl−methyl distance between opposite layers being 3.936 and 3.927 Å in the crystal lattices of NLBA and NMBA, respectively. The van der Waals distance between the methyl groups in the same leaflet are 4.861 and 4.866 Å for NLBA and NMBA, respectively. The bilayer thickness (i.e., Me–Me distance) in the crystal lattices of NLBA and NMBA are 32.78 and 36.96 Å, respectively, and the monolayer (single leaflet) thickness (O3−C12 distance) for NLBA is 16.11 Å and for NMBA (O3–C14 distance) it is 18.19 Å. The repeat distance (*d*-spacing) is 35.56 and 39.06 Å for NLBA and NMBA, respectively. The *N*-acyl chains are tilted by 33.28° (in NLBA) and 34.42° (in NMBA) with respect to the bilayer normal. This is in contrast to the situation found in the crystals of N-acylglycines, in which the acyl chains are essentially perpendicular to the bilayer plane.[31] This shows that the additional CH_2 unit in the head group significantly affects the crystal packing in NABAs.

3.7. Hydrogen bonding

Two different views of hydrogen bonding pattern in the crystal structure of NMBA are shown in Fig. 6C,D. These figures show that hydrogen bonds between carboxylic acid moieties of opposing layers form 8-membered cyclic structures through O—H···O hydrogen bonds, with each carboxylic acid group acting both as a proton donor as well as a proton acceptor. The H···O distances in the O—H···O hydrogen bonds and the bond angles subtended at the hydrogen atom for NLBA and NMBA are 1.833 Å, 1.829 Å, 175.31° and 173.86°, respectively. The distance between donor and acceptor oxygen atoms for NLBA and NMBA are 2.65 and 2.646 Å, respectively. Besides the hydrogen bonds between the carboxyl groups, strong hydrogen bonds are also formed between the amide N—H and carbonyl oxygen of adjacent NMBA molecules (Fig. 6C). While the N—H group of each NMBA molecule forms a hydrogen bond with another NMBA molecule in the adjacent unit cell on one side, the carbonyl oxygen of the same molecule forms a hydrogen bond with the amide N−H of another NMBA molecule in the adjacent unit cell on the other side (Fig. 6D). All these hydrogen bonds are also identical, with a N—O distance of 2.902 and 2.908 Å, a H···O distance of 2.064 and 2.072 Å, and a N—H···O angle of 164.69 and 164.07°, respectively, for NLBA and NMBA. Similar N—H···O hydrogen bonds have been observed in a number of other amphiphiles bearing *N*-acyl chains, viz., *N*-acyldopamines, *N*-acylglycines, *N*-acylethanolamines, *N*-palmitoylpropanolamine, *N*, *O*-diacylethanolamines and a C3-symmetric triamide with three alkyl chains (Reddy et al., 2014, 2013; Kamlekar et al., 2010; Tarafdar et al., 2012; Dahlen et al., 1977; Ramakrishnan and Swamy, 1999; Kamlekar and Swamy, 2006; Rudert et al., 1996; Hou et al., 2012).

3.8. Powder X-ray diffraction

In order to compare the structures of even-chainlength and odd-chainlength NABAs, we tried to get single crystals of odd-chain NABAs bearing short as well as long acyl chains; however, these attempts did not yield any success. Therefore we have carried

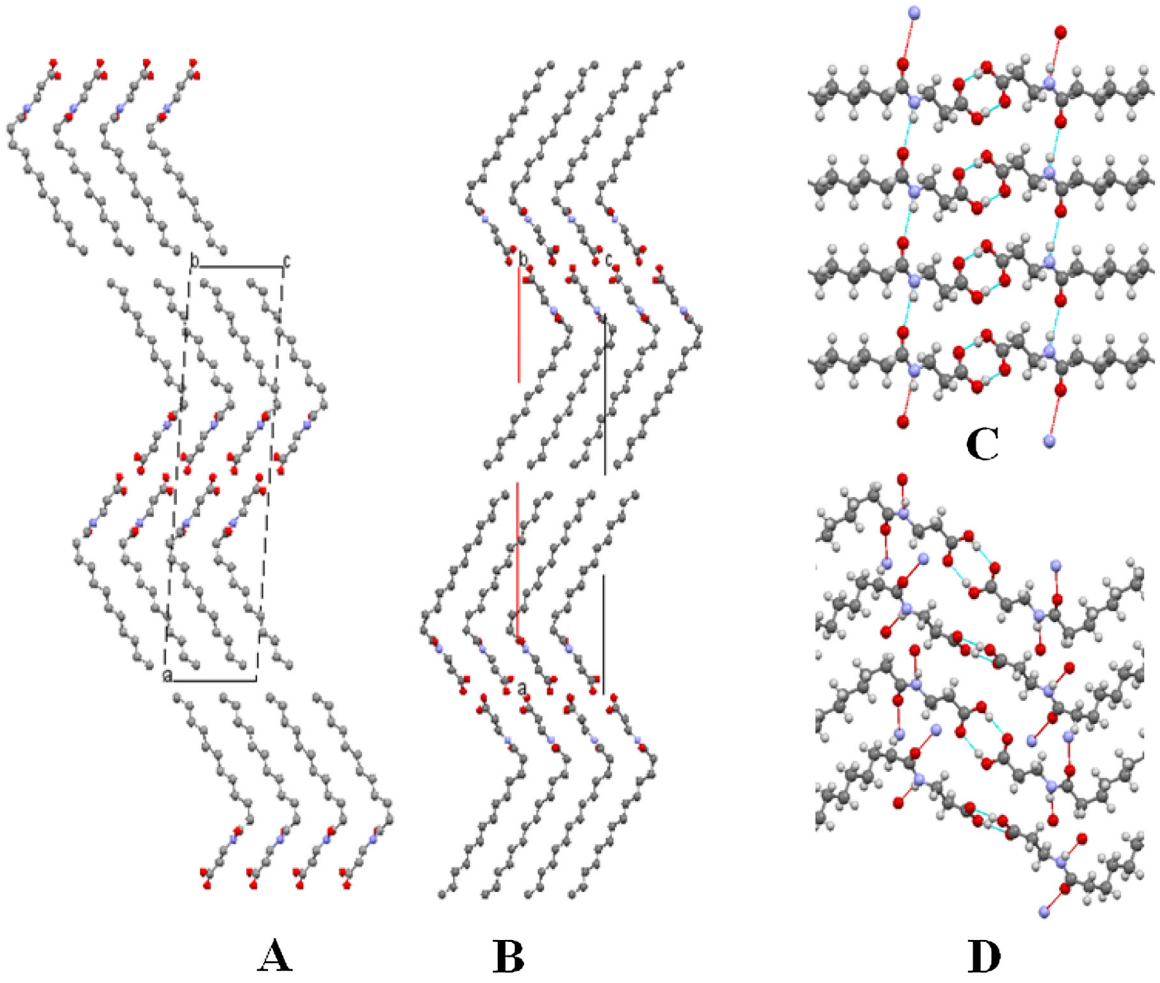

Fig. 6. Packing diagrams of (A) *N*-lauroyl-β-alanine and (B) *N*-myristoyl-β-alanine along the *b*-axis. (C, D) Two different views of the hydrogen bonding pattern in the crystal lattice of NMBA.

out powder X-ray diffraction studies in order to derive some structural information on the entire chainlength series. The PXRD data obtained with NABAs of different chainlengths are shown in Fig. 7A,B. All NABAs (n = 8–20) gave several sharp diffraction peaks in the 2θ range of 1–30° and the *d*-spacing values for all NABAs were calculated from the powder diffraction peak positions using Bragg's equation. In each case 4–6 peaks were used to estimate the *d*-spacings and average values are given in Table S15. The corresponding plot of chain length dependence of the *d*-spacing is shown in Fig. 7C. Interestingly, odd-even alteration is seen in the *d*-spacing values, with the odd-chain NABAs showing higher values as compared to the even-chain molecules. Such odd-even alteration in the *d*-spacings was not observed previously in any homologous series of single chain amphiphiles. The *d*-spacings of both odd- and even-chainlength compounds independently exhibit an essentially linear dependence on the chainlength with a slope of 2.414 and 2.006 Å/CH_2, which correspond to increments of 1.207 and 1.003 Å per additional CH_2 moiety, respectively.

If the molecules were to pack in a normal bilayer format, the *d*-spacing value would be 2.54 Å, when the acyl chain length is increased by one CH_2 unit and each CH_2 group increases the *d*-spacing by 1.27 Å. In comparison, the incremental *d*-spacings estimated from the PXRD data are significantly smaller for the even-chain NABAs and somewhat smaller for the odd-chain NABAs. Therefore, the acyl chains in both odd-chain and even-chain NABAs must be tilted with respect to the bilayer normal but to different extents for the two series, with the odd chain length series having a smaller tilt angle. In agreement with this, the acyl chain tilt angles with respect to the bilayer normal for odd- and even chain length series were calculated from the above slopes as 18.14 and 37.83° respectively.

4. Summary and conclusions

The present work reports the thermotropic phase behavior and supramolecular organization of a homologous series of *N*-acyl-β-alanines, which are homologues of *N*-acyl glycines and *N*-acyl GABAs, which act as signaling molecules in mammalian brain. DSC studies on dry and hydrated (with water) NABAs revealed changes in the polymorphic forms in successive heating scans. DSC studies of NABAs hydrated with buffer of pH 7.6 (carboxylate/anionic form) showed only a single transition, whereas minor transitions were seen in the dry state and upon hydration with water (acid/neutral form). Transition enthalpies and entropies of dry and hydrated (with buffer) samples showed linear dependence on chain length, whereas odd-even alternation was observed when hydrated with water. Crystal structures of *N*-lauroyl-β-alanine and *N*-myristoyl-β-alanine revealed tilted bilayer packing of the acyl chains, which is similar to the packing observed in *N*-acylethanolamines. PXRD measurements showed odd-even alternation in the *d*-spacings, which was not observed earlier in single and double chain amphiphiles. These results show that additional methylene group in the head group changes both three dimensional structures and thermodynamics of phase transitions of NABAs as compared to *N*-

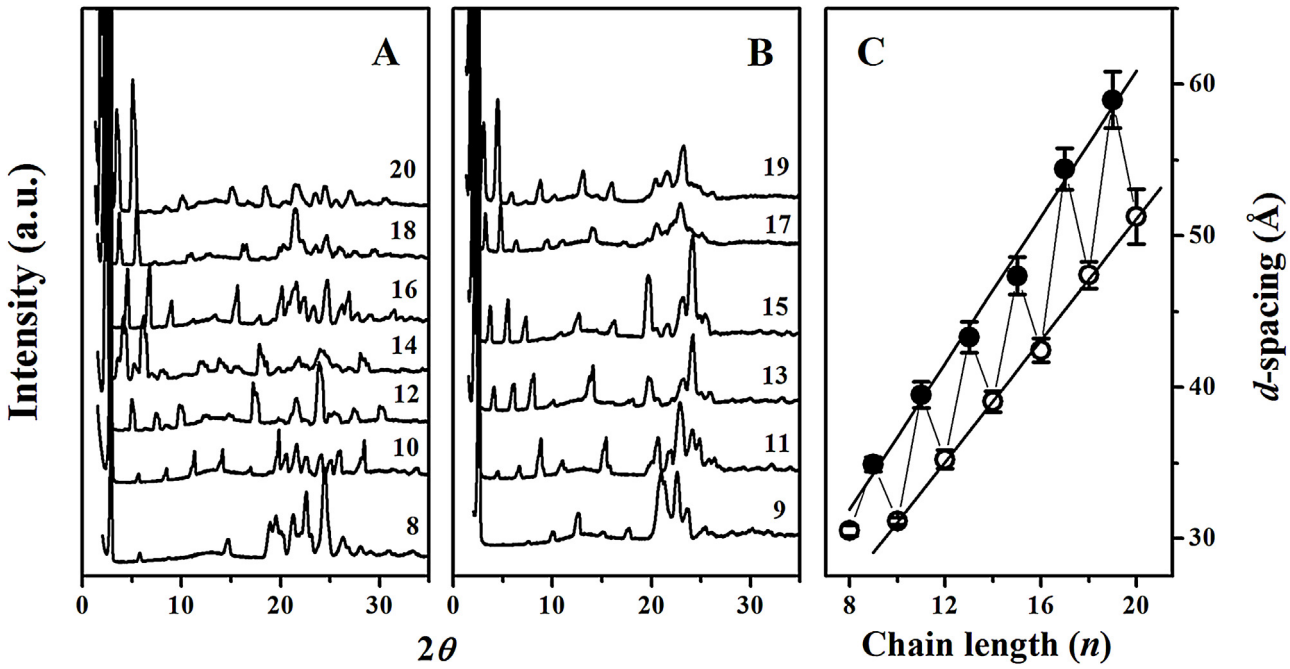

Fig. 7. Powder X-ray diffraction patterns of *N*-acyl-β-alanines with different saturated acyl chains (A, B) and chain length dependence of *d*-spacings (C). The number of C-atoms in the acyl chain of the NABAs is indicated against the corresponding PXRD profiles. In panel C, solid lines represent linear least squares fits for the odd (●) – and even (O) chain length NABAs. The slopes of the lines yielded increase in the *d*-spacing per each additional CH_2 group as 2.414 and 2.006 Å, respectively, for the odd- and even-chain length NABAs.

acylglycines.[31] Changes observed in the polymorphic behavior upon first heating and odd-even alteration in *d*-spacings indicate that the phase behavior of NABAs is complex and merit further investigations on the three dimensional structure of different polymorphs. Such studies are currently underway in our laboratory.

Acknowledgements

This work was supported by a research grant from the Department of Science and Technology (India) to MJS. DS was supported by a Senior Research Fellowship from the Council of Scientific and Industrial Research (India). Use of the National Single Crystal Diffractometer Facility (SMART APEX CCD single crystal X-ray diffractometer) at the School of Chemistry, University of Hyderabad, funded by the Department of Science and Technology (India) is gratefully acknowledged. The University Grants Commission (India) is acknowledged for their support through the UPE and CAS programs, to the University of Hyderabad and School of Chemistry, respectively.

Appendix A. Supplementary data

Supplementary data associated with this article can be found, in the online version, at http://dx.doi.org/10.1016/j.chemphyslip.2016.10.002.

References

Akoka, S., Tellier, C., Le Roux, C., Marion, D., 1988. A phosphorus magnetic resonance spectroscopy and a differential scanning calorimetry study of the physical properties of *N*-acylphosphatidylethanolamines in aqueous dispersions. Chem. Phys. Lipids 46, 43–50.

Bradshaw, H.B., Rimmerman, N., Krey, J.F., Walker, J.M., 2006. Sex and hormonal cycle differences in rat brain levels of pain-related cannabimimetic lipid mediators. Am. J. Physiol. Regul. Inter. Comp. Physiol. 291, R349–R358.

Bradshaw, H.B., Rimmerman, N., Hu, S.S.-J., Benton, V.M., Stuart, J.M., Masuda, K., Cravatt, B.F., O'Dell, D.K., Walker, J.M., 2009. The endocannabinoid anandamide is a precursor for the signaling lipid *N*-arachidonoyl glycine by two distinct pathways. BMC Biochem. 10, 14.

Cascio, M.G., Minassi, A., Ligresti, A., Appendino, G., Burstein, S., Di Marzo, V., 2004. A structure activity relationship on *N*-arachidonoyl amino acids as possible endogenous inhibitors of fatty acid amide hydrolase. Biochem. Biophys. Res. Commun. 314, 192–196.

Chu, C.J., Huang, S.M., De Petrocellis, L., Bisogno, T., Ewing, S.A., Miller, J.D., Zipkin, R. E., Daddario, N., Appendino, G., Di Marzo, V., Walker, J.M., 2003. *N*-oleoyldopamine, a novel endogenous capsaicin-like lipid that produces hyperalgesia. J. Biol. Chem. 278, 13633–13639.

Curtis, D.R., Hosli, L., Johnston, G.A.R., 1968. A pharmacological study of the depression of spinal neurons by glycine and related amino Acids. Exp. Brain Res. 6, 1–18.

Dahlen, B., Pascher, I., Sundell, S., 1977. The crystal structure of *N*-(2-hydroxyethyl)-octadecanamide. Acta Chem. Scand. A 31, 313–320.

Davidoff, R.A., Aprison, M.A., Werman, R., 1969. The effects of strychnine on the inhibition of interneurons by glycine and γ-aminobutyric acid. Neuropharmacology 8, 191–194.

Derave, W., Ozdemir, M.S., Harris, R.C., Pottier, A., Reyngoudt, H., Koppo, K., Wise, J. A., Achten, E., 2007. β-Alanine supplementation augments muscle carnosine content and attenuates fatigue during repeated isokinetic contraction bouts in trained sprinters. J. Appl. Physiol. 103, 1736–1743.

Duarte, R.C., Ongaratto, R., Piovesan, L.A., Lima, V.R., Soldi, V., Merlo, A.A., D'Oca, G. M., 2012. New N-acylamino acids and derivatives from renewable fatty acids: gelation of hydrocarbons and thermal properties. Tetrahedron Lett. 53, 2454–2460.

Guo, J., Williams, D.J., Ikeda, S.R., 2008. *N*-arachidonyl L-serine, A putative endocannabinoid, Alters the activation of *N*-type calcium channels in sympathetic neurons. J. Neurophysiol. 100, 1147–1151.

Harris, R.C., Tallon, M.J., Dunnett, M., Boobis, L., Coakley, J., Kim, H.J., Fallowfield, J.L., Hill, C.A., Sale, C., Wise, J.A., 2006. The absorption of orally supplied β-alanine and its effect on muscle carnosine synthesis in human vastus lateralis. Amino Acids 30, 279–289.

Hill, C.A., Harris, R.C., Kim, H.J., Harris, B.D., Sale, C., Boobis, L.H., Kim, C.K., Wise, J.A., 2007. Influence of β-alanine supplementation on skeletal muscle carnosine concentrations and high intensity cycling capacity. Amino Acids 32, 225–233.

Horikoshi, T., Asanuma, A., Yanagisawa, K., Anzai, K., Goto, S., 1988. Taurine and β-alanine act on both GABA and glycine receptors in *Xenopus oocyte* injected with mouse brain messenger RNA. Mol. Brain Res. 4, 97–105.

Hou, X., Schober, M., Chu, Q., 2012. A chiral nanosheet connected by amide hydrogen bonds. Cryst. Growth Des. 12, 5159–5163.

Huang, S.M., Bisogno, T., Petros, T.J., Chang, S.-Y., Zavitsanos, P.A., Zipkin, R.E., Sivakumar, R., Coop, A., Maeda, D.Y., De Petrocellis, L., Burstein, S., Di Marzo, V., Walker, J.M., 2001. Identification of a new class of molecules, the arachidonyl

amino acids, and characterization of one member that inhibits pain. J. Biol. Chem. 276, 42639–42644.
Kamlekar, R.K., Swamy, M.J., 2006. Molecular packing and intermolecular interactions in two structural polymorphs of *N*-palmitoylethanolamine, a type 2 cannabinoid receptor agonist. J. Lipid Res. 47, 1425–1433.
Kamlekar, R.K., Tarafdar, P.K., Swamy, M.J., 2010. Synthesis, calorimetric studies, and crystal structures of *NO*-diacylethanolamines with matched chains. J. Lipid Res. 51, 42–52.
Larsson, K., 1986. In: Gunstone, F.D., Harwood, F.D., Padley, J.L. (Eds.), The Lipid Handbook. Chapman and Hall, London, pp. 321–384.
Lewis, R.N.A.H., Sykes, B.D., McElhaney, R.N., 1987. Thermotropic phase behavior of model membranes composed of phosphatidylcholines containing *dl*-methyl anteisobranched fatty Acids. 1. Differential scanning calorimetric and ^{31}P-NMR spectroscopic studies. Biochemistry 26, 4036–4044.
Lewis, R.N.A.H., Mantsch, H.H., McElhaney, R.N., 1989. Thermotropic phase behavior of phospatidylcholines with ώ-tertiary-butyl fatty acyl chains. Biophys. J. 56, 183–193.
Ma, C.-Y., Paquet, A., McKellar, R.C., 1993. Effect of fatty *N*-acyl amino acids on some functional properties of two food proteins. J. Agric. Food Chem. 47, 1182–1186.
Marsh, D., 1982. Biomembranes. In: Pifat, G., Herak, J.N. (Eds.), Supramolecular Structure and Function. Plenum Press, New York, pp. 127–178.
Marsh, D., 1990. Handbook of Lipid Bilayers. CRC Press, Boca Raton, FL.
Milman, G., Maor, Y., Abu-Lafi, S., Horowitz, M., Gallily, R., Baktai, S., Mo, F.-M., Offeretaler, L., Pacher, P., Kunos, G., Mechoulam, R., 2006. *N*-arachidonyl L-serine, An endocannabinoid-like brain constituent with vasodilatory properties. Proc. Natl. Acad. Sci. U. S. A. 103, 2428–2433.
Mori, M., Gahwiler, B.H., Gerber, U., 2002. β-alanine and taurine as endogenous agonists at glycine receptors in rat hippocampus *in vitro*. J. Physiol. 539 (1), 191–200.
Murase, H., Nagao, A., Terao, J., 1993. Antioxidant and emulsifying activity of *N*-(Long-chain-acyl)histidine and *N*-(Long-chain-acy1) carnosine. J. Agric. Food Chem. 41, 1601–1604.
Ramakrishnan, M., Swamy, M.J., 1998. Differential scanning calorimetric studies on the thermotropic phase transitions of *N*-acylethanolamines of odd chainlengths. Chem. Phys. Lipids 94, 43–51.
Ramakrishnan, M., Swamy, M.J., 1999. Molecular packing and intermolecular interactions in *N*-acylethanolamines: crystal structure of *N*-myristoylethanolamine. Biochim. Biophys. Acta 1418, 261–267.
Ramakrishnan, M., Sheeba, V., Komath, S.S., Swamy, M.J., 1997. Differential Sscanning calorimetric studies on the thermotropic phase transitions of dry and hydrated forms of *N*-acylethanolamines of even chainlengths. Biochim. Biophys. Acta 1329, 302–310.
Reddy, S.T., Swamy, M.J., 2015. Synthesis, physicochemical characterization and membrane interactions of a homologous series of *N*-acylserotonins: bioactive, endogenous conjugates of serotonin with fatty acids. Biochim. Biophys. Acta 1848, 95–103.
Reddy, S.T., Tarafdar, P.K., Kamlekar, R.K., Swamy, M.J., 2013. Structure and thermotropic phase behavior of a homologous series of bioactive *N*-acyldopamines. J. Phys. Chem. B 117, 8747–8757.
Reddy, S.T., Krovi, K.P., Swamy, M.J., 2014. Structure and thermotropic phase behavior of a homologous series of *N*-acylglycines: neuroactive and antinociceptive constituents of biomembranes. Cryst. Growth Des. 14, 4944–4954.
Rimmerman, N., Bradshaw, H.B., Hughes, H.V., Chen, J.S.-C., Hu, S.S.-J., McHugh, D., Vefring, E., Jahnsen, J.A., Thompson, E.L., Masuda, K., Cravatt, B.F., Burstein, S., Vasko, M.R., Prieto, A.L., O'Dell, D.K., Walker, J.M., 2008. *N*-palmitoyl glycine, A aovel endogenous lipid that acts as a modulator of calcium influx and nitric oxide production in sensory neurons. Mol. Pharmacol. 74, 213–224.
Rudert, R., Wu, Y., Vollhardt, D., 1996. The crystal structure of *N*-(3-hydroxypropyl)-hexadecanoic acid amide. Z. Kristallogr. 211, 114–116.
Saghatelian, A., Mckinney, M.K., Babdell, M., Patapoutian, A., Cravatt, B.F., 2006. A FAAH-regulated class of *N*-acyl taurines that activates TRP ion channels. Biochemistry 45, 9007–9015.
Schmieden, V., Kuhse, J., Betz, H., 1993. Mutation of glycine receptor subunit creates β-alanine reeceptor responsive to GABA. Science 262, 256–258.
Sivaramakrishna, D., Swamy, M.J., 2015a. Differential scanning calorimetric and powder x-ray diffraction studies on a homologous series of *N*-acyl-L-alanine esters with matched Chains (*n* = 9-18). J. Chem. Sci 127, 1627–1635.
Sivaramakrishna, D., Swamy, M.J., 2015b. Self-Assembly, supramolecular organization, and phase behavior of L-Aalanine alkyl esters (n = 9-18) and characterization of equimolar L-alanine lauryl ester/Lauryl sulfate catanionic complex. Langmuir 31, 9546–9556.
Sivaramakrishna, D., Swamy, M.J., 2016. Synthesis, characterization and thermotropic phase behavior of a homologous series of *N*-acyl-L-alaninols and interaction of *N*-myristoyl L-alaninol with dimyristoylphosphatidylcholine. Chem. Phys. Lipids 196, 5–12.
Sivaramakrishna, D., Reddy, S.T., Nagaraju, T., Swamy, M.J., 2015. Self-assembly, supramolecular organization and phase transitions of a homologous series of *N*-acyl-L-alanines (n = 8–20). Colloids Surfaces A: Physicochem. Eng. Aspects 471, 108–116.
Smith, E.C.B., 1938. The buffering of muscle in rigor; protein, phosphate and carnosine. J. Physiol. 92, 336–343.
Tan, B., O'Dell, D.K., Yu, Y.W., Monn, M.F., Hughes, H.V., Burstein, S., Walker, J.M., 2010. Identification of endogenous acyl amino acids based on a targeted lipidomics approach. J. Lipid Res. 51, 112–119.
Tarafdar, P.K., Reddy, S.T., Swamy, M.J., 2012. Nonclassical odd-even alternation in mixed-chain diacylethanolamines: implications of polymorphism. Cryst. Growth Des. 12, 1132–1140.
Vintiloiu, A., Lafleur, M., Bastiat, G., Leroux, J.C., 2008. In situ-forming oleogel implant for rivastigmine Delivery. Pharm. Res. 25, 845–852.
Wiles, A.L., Pearlman, R.-J., Rosvall, M., Aubrey, K.R., Vandenberg, R.J., 2006. *N*-arachidonyl glycine inhibits the glycine transporter, GLYT2a. J. Neurochem. 99, 781–786.